5
Stator winding fault diagnosis

5.1 INTRODUCTION

One of the main causes of motor breakdown is the failure of insulation in the stator windings. With the insulation failure, the faults in the stator can grow to serious faults, which are hazardous for the motor. The faults share about 30-40% of total motor faults [Group et al., 1987; Thorsen and Dalva, 1995]. The general cause of insulation failure is the breaking of turn to turn insulation or shorting between turns [Grubic et al., 2008; Siddique et al., 2005]. It is caused due to a combination of effects including vibrations caused by electromechanical forces, frequent motor start-ups and stops, high dv/dt voltage surges, mechanical stresses, thermal overload, and/or contamination.

The long persistence of local shorting of turns may lead to coil to coil faults, phase to coil faults and ground faults. These faults are very severe and can burn off the motor winding within no time. Thus, monitoring of the stator winding inter-turn shorts at an early stage of inception is of prime importance.

For high voltage motors up to $4kV$, the partial discharge based methods are utilized for stator related faults. However, for low-voltage motors, the fault detection methods are still in the process of finalization [Sharifi and Ebrahimi, 2011]. Nevertheless, in general, there is some lead time between turn-shorts to complete failure in case of low-voltage motors [Jover Rodriguez and Arkkio, 2008]. This lead time is sufficient enough for diagnostic techniques to detect shorting of turns in the motor. The timely detection of fault would help in scheduling maintenance in advance without compromising with the production and financial intricacies. Thus, an efficient fault diagnostic algorithm for stator winding fault is an essential requirement for the induction motor protection.

It has been reported in [Thomson and Morrison, 2002] that the frequency components in the air-gap flux arise due to stator shorted turns, that can be observed in the current spectrum. These components in the air-gap flux are given by the following Equation 5.1:

$$f_a = \left[\frac{n}{p}(1-s) \pm k\right] f_m \tag{5.1}$$

where, f_a are the frequency components arise due to shorting, f_m is the supply frequency, p is the pair of poles, s is the slip, $n = 1,2,3...$ and $k = 1,3,5....$ For different values of n and k, the fault frequency components are calculated and provided in Table 5.1. The frequencies 25 Hz and 75 Hz

Table 5.1 : Harmonics present due to stator winding inter-turn faults

$n\|k$	1	3	5
1	75/25 Hz	125/25 Hz	175/75 Hz
2	100/0 Hz	200/150 Hz	300/200 Hz
3	125/25 Hz	225/75 Hz	325/175 Hz

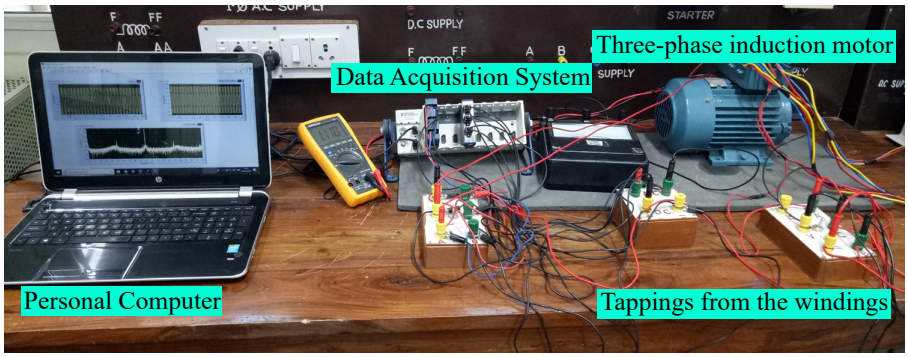

Figure 5.1 : Experimental set-up to record current signals for stator winding fault diagnosis

cannot be utilized for fault diagnostic purposes as they also arise due to machine asymmetries present in healthy conditions also. It has been reported that stator turn faults affect twice the supply frequency, i.e. 100 Hz, but, this frequency is also affected by other variations in the machine dynamics such as load variations. The frequencies 125 Hz and 175 Hz are found to be varying with the turn-faults [Thomson and Morrison, 2002], thus, can be used for the analysis of stator winding faults. Also, other frequencies like 225 Hz and higher can also been used.

The stator winding faults considered under the present study are, stator winding inter-turn faults and phase to ground faults. With the help of Stockwell transform, the stator current signals are decomposed into complex ST matrix whose magnitude has been utilized for the fault detection. After fault detection, discrimination between the turn-faults and the ground faults is performed with the help of zero sequence currents. Following this, two Support Vector Machine (SVM) models are used to identify the location of the fault i.e., the faulty phase for both turn-faults and ground faults. The features in specific frequency bands determined by Table 5.1 are used as input to the SVM to detect faulty phase in case of turn-faults. For ground faults, features are extracted in a wider frequency bands as input to the SVM model. Under both cases, a heuristic feature selection approach is utilized to find the optimal features for classification purpose. A good classification is achieved for both types of faults.

5.2 EXPERIMENTAL SET-UP

A three-phase induction motor ratings 0.75 kW (1 HP), 415 V, 4-pole, 50 Hz, 2 Amp, 1380 rpm has been used under the experimental study. The rotor is suspended with two bearings viz. 6204 ZZ and 6203 ZZ. The motor is run under no-load conditions. For reference, the current signals for a healthy motor (without any fault) are recorded. The experimental hardware set-up used for the study is shown in Figure 5.1. The faults in the windings are emulated in the motor. To create turn-faults, wires are soldered on the three adjacent turns of the middle of each phase winding. The ends of these wires are taken out as taps on the panel mounted over the top of the motor. This way there are three turns per phase i.e. nine taps available for experiments of turn-faults. For the ground faults, a wire-end is taken out from the stator core and mounted over the top of the motor.

The current signals are recorded using National Instruments based data acquisition system which comprises of NI-9178 chassis, NI-9247 current module (50 A) and an interfacing LabVIEW software with the personal computer. The sampling rate was set at 6.4 kHz.

Since, there are three taps available for a single phase winding of the motor, three turn-shorts can be emulated for three phases. Suppose, if A1, A2 and A3 are three taps of phase-A, then shorting between A1-A2, A2-A3 and A1-A3 are conducted and current data is recorded. Thus,

there are nine cases of turn-shorts performed. For ground faults, each turn-tapping is shorted with ground connection (G) taken out from stator core through a shorting resistor (R). The details of this winding faults emulated is shown in Table 5.2. Stator current signals are recorded under both case studies with proper annotation of location of the corresponding faulty phase. In each experiment, a sample is recorded consisting of all three-phase current signals.

Table 5.2 : Details of the emulated stator winding faults

Fault Type	Details
Turn faults	taps from three adjacent turns total nine taps available 1.6% turns shorted at a time nine possible combinations of turn-shorts
Ground faults	nine connections to ground through shorting resistor (R) R = 500 kΩ 100 kΩ 50 kΩ 10 kΩ 5 kΩ 1000 Ω 500 Ω

5.3 STATOR WINDING FAULT DIAGNOSIS

The stator current signals recorded for all conditions of stator windings (healthy, turn-faults and ground faults) in a three-phase induction motor are shown in Figure 5.2. Spectral analysis is performed using FFT to identify the variation of frequencies in different conditions of the motor. The FFT of stator current signals for phase-A and phase-B are shown in Figure 5.3 respectively.

It can be observed that under the faults in the stator winding has changed the current spectrum as evident from the Figure 5.3. The quantification of these changes is difficult due to limitations of FFT. Thus, multi-resolution based analysis using Stockwell transform would be useful in extracting information in the time-frequency plane.

Stockwell transform is used to analyse the stator current signals recorded under various conditions of winding faults. A complex matrix with information in both time and frequency is obtained. Various statistical properties are calculated for the magnitude of the ST matrix. These properties include mean, maximum, standard deviation, kurtosis, mean absolute deviation, skewness, energy and entropy. The most discriminating characteristics were found in the standard deviation (SD) of the magnitude of ST matrix obtained with respect to frequency axis. Subsequently, SD is used as a fault diagnostic parameter in the proposed algorithm. The algorithm consists of following steps:

1. Fault detection
2. Distinguishing turn-faults from ground-faults
3. Detection of faulty phase in turn-faults
4. Detection of faulty phase in ground-faults

5.3.1 Winding Fault detection

For the detection of a fault, the standard deviation of each phase for all frequencies has been calculated. A frequency range is set according to Equation 5.1 and Table 5.1. Three frequencies have been utilized, 125 Hz, 175 Hz and 225 Hz for the fault detection. To encompass the minor

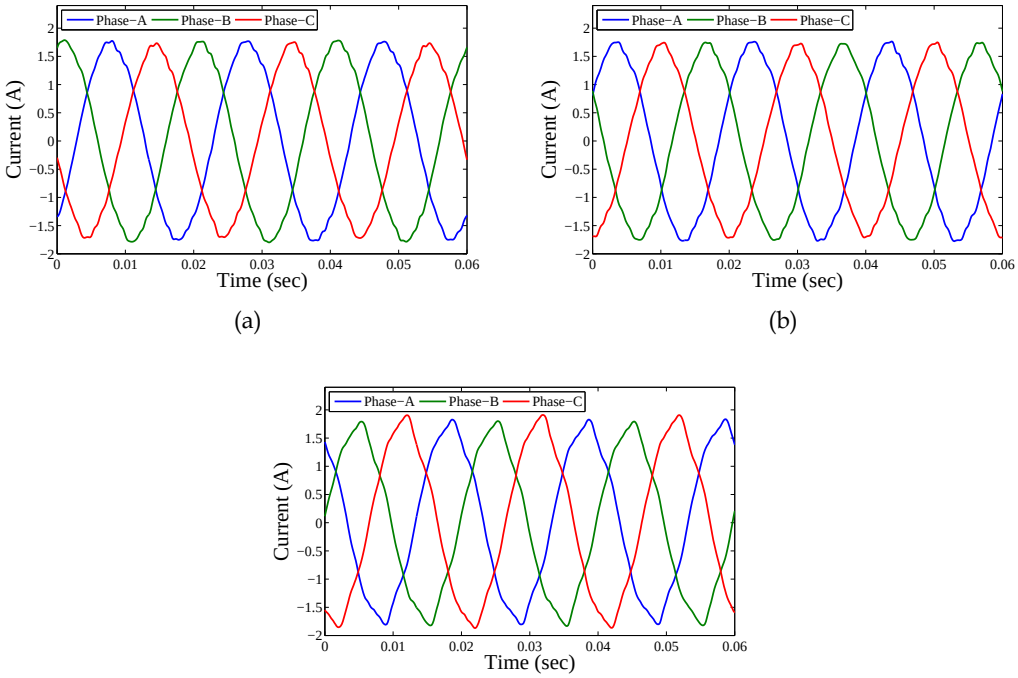

Figure 5.2 : Stator current signals for (a) healthy, (b) turn-fault, and (c) ground fault for a three-phase induction motor

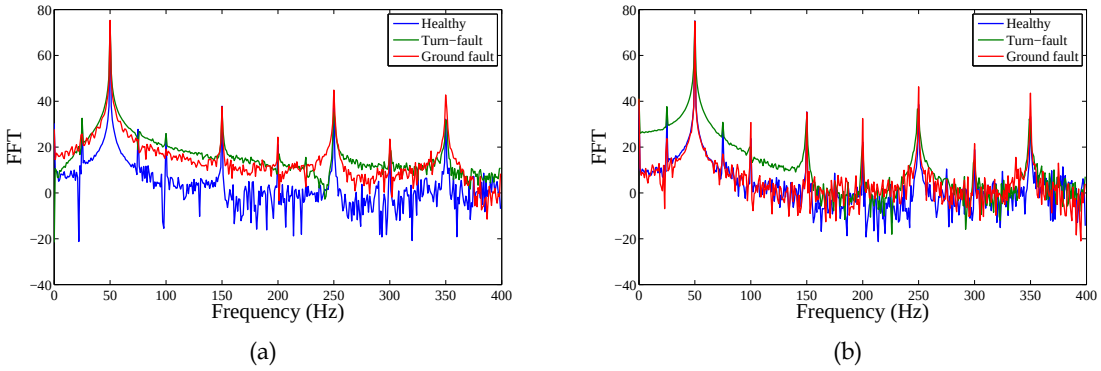

Figure 5.3 : FFT of stator current signals of (a) Phase-A, and (b) Phase-B under healthy, turn-fault and ground faults conditions

fluctuations around these frequencies, the narrow bands centred around the chosen frequencies are defined. Frequencies ranging between $\pm$ 10 Hz around the above-mentioned frequencies are taken into consideration. Therefore, the resultant frequency ranges are $Fr_1 = [115 - 135]$ Hz, $Fr_2 = [165 - 185]$ Hz, and $Fr_3 = [215 - 225]$ Hz. The SD of magnitude matrices is calculated under these pre-defined frequency ranges. Based on the SDs of each phase, the first fault index for detection of fault is defined in Equation 5.2:

$$FI_1 = \sum_{i=1}^{3} std(|S_i(\tau, f)|))|_{Fr_1, Fr_2, Fr_3} \tag{5.2}$$

where, $S_i(\tau, f)$ is the ST matrix for i^{th} phase and $i = 1, 2, 3$ for all three phases. Thus, the fault index (FI_1) includes the summation of standard deviation of magnitude matrices for three phases. Using this index, detection of fault (turn-shorts or ground-fault) can be performed.

5.3.2 Discrimination of turn-faults from ground-faults

Post fault detection, the following step is to identify whether the cause of the fault is due to turn-faults or ground-fault. For this purpose, the second fault index based on zero-sequence current has been defined. Zero sequence currents (I_0) are prominent in case of the ground faults in the motor. This can be utilized in distinguishing turn-shorts and ground faults. Based on this, the fault index, FI_2 is defined in Equation 5.3:

$$FI_2 = std(|I_0|) \tag{5.3}$$

where, I_0 is the zero sequence current and is given as, $I_0 = (I_a + I_b + I_c)/3$, and I_a, I_b, I_c are the phase currents of winding A, B and C respectively. Once the type of fault is identified as turn-faults or ground-faults, the objective is to identify the faulty phase. For this purpose, a machine learning based approach using two SVM models, for each fault type has been proposed. The detailed methodologies for both classification strategies are explained in the following sub-sections.

5.3.3 Detection of faulty phase with turn-faults

The faulty phase is identified with the help of a classifier based on the features extracted from ST matrix of each sample of fault (consisting of three-phase current signals). Feature extraction and selection is followed by classification into three fault classes.

Feature extraction

For the classification purposes, the features are curated from the SD of the magnitude of ST matrix calculated for current signals of each phase. The SD is obtained for the selected frequency ranges, Fr_1, Fr_2, and Fr_3 identified in Section 5.3.1 which are the presumed to be affected by winding faults. These ranges are termed as, $Fr_1^1 = 115$ Hz, $Fr_1^2 = 135$ Hz, $Fr_2^1 = 165$ Hz, $Fr_2^2 = 185$ Hz, $Fr_3^1 = 215$ Hz, and $Fr_3^2 = 225$ Hz. The SD is calculated within these frequency ranges for each phase ST matrix, followed by the features formation given as:

$$feat_n = \sum_{Fr_i^1}^{Fr_i^2} std(|S_j(\tau, f))| \tag{5.4}$$

where, fea_n is the n^{th} feature with $n = 1, 2, 3, ..9$, $i = 1, 2, 3$ is the chosen three frequency ranges and $j = 1, 2, 3$ representing three-phases phase-A, phase-B and phase-C respectively. Thus, for each sample of fault with three phase current signals, there are nine features to represent the fault. The details of the features are provided in Table 5.3.

Feature selection and classification

Not all features might be useful for the purpose of classification. Therefore, selection of relevant features is an important task before feeding them to the classifier. For this reason, a heuristic approach is utilized where all possible combinations of n features ($n = 2, 3, 4....9$ is number of features) are trained and tested. Thus, a total of $C_n^9 \sim C_2^9 + C_3^9 + ...C_9^9 = 502$ combinations are fed to SVM, the one with the best accuracy is utilized. This is performed as per follows:
Step 1: Initialize $n = 2$, and make the feature set with first n features.
Step 2: Compute the classification accuracy using SVM.
Step 3: If the accuracy is less than 100%, take another combination of n features.

Table 5.3 : Features list for faulty phase detection in turn-faults

Feature Name	Phase	Frequency range
$feat_1$	A	Fr_1
$feat_2$	A	Fr_2
$feat_3$	A	Fr_3
$feat_4$	B	Fr_1
$feat_5$	B	Fr_2
$feat_6$	B	Fr_3
$feat_7$	C	Fr_1
$feat_8$	C	Fr_2
$feat_9$	C	Fr_3

Step 4: Repeat the above procedure with $n = n+1$ till all features are exhausted. The whole process of feature extraction, selection and classification has been illustrated in Figure 5.4

5.3.4 Detection of faulty phase with ground-faults

In order to detect the faulty phase, in case of ground faults, another SVM model is trained. For this purpose, the features are extracted from ST matrix, followed by heuristic feature selection using SVM to identify the faulty phase i.e., phase-A fault, phase-B fault and phase-C fault. These steps are detailed in the following sub-sections below:

Feature Extraction

The ground faults are emulated in the experiments with the help of various shorting resistors as mentioned as detailed in Table 5.2. There were 189 samples collected with all resistors such that 63 samples were collected pertaining to each fault class. The features were extracted from the SD of magnitude of ST matrix for each phase current. Figure 5.5 (a), (b), and (c) show the standard deviation plots for ground faults in phase-A, phase-B and phase-C respectively.

It can be observed that at specific frequency ranges (highlighted), the values of SD for the faulty phase are higher as compared to other phases. These frequency ranges are either different or coincide for all three locations of faults. This is due to the reason that fault in one phase affects the currents in other phases, as neutral current flows back in the phases through the ground. This causes a simultaneous effect on other phases also. This inter-phase effect does not change a small set of frequencies in the faulty phase which leads to a wider range of frequencies getting affected due to the ground faults. To encompass all such fault affected frequency ranges, a set of frequency ranges are chosen on the basis of observation done for many samples of fault. First, frequencies are identified for each faulty phase such that only that phase has higher SD values than other phases. Based on individual frequency ranges for each phase, the final frequency ranges are selected such that all useful frequencies are covered for all three-phases. All these frequency ranges are shown in Table 5.4. Thus, the final frequency ranges are named as $f1$ = [280-350 Hz], $f2$=[100-120 Hz], and $f3$=[190-240 Hz]. The features extracted within these frequency ranges for each phase are given

Table 5.4 : Frequency ranges useful for detecting the faulty phase

Faulty Phases	Useful frequency ranges	Selected frequency ranges
Phase-A	300-350 Hz	280-350 Hz, 100-120 Hz, 190-240 Hz
Phase-B	90-120 Hz, 280-350 Hz	
Phase-C	100-160 Hz, 190-240 Hz	

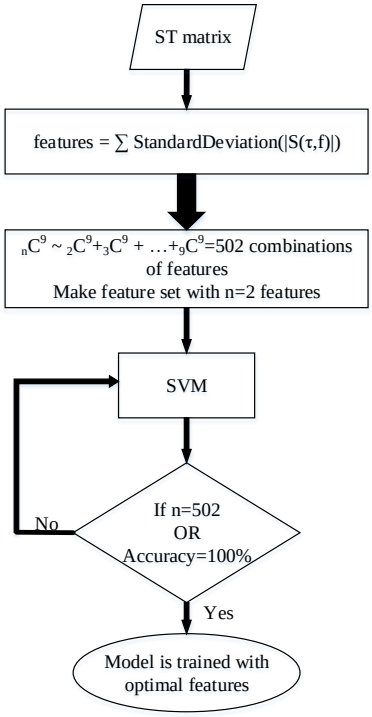

Figure 5.4 : Block diagram summarizing feature extraction, selection and classification process for stator faults

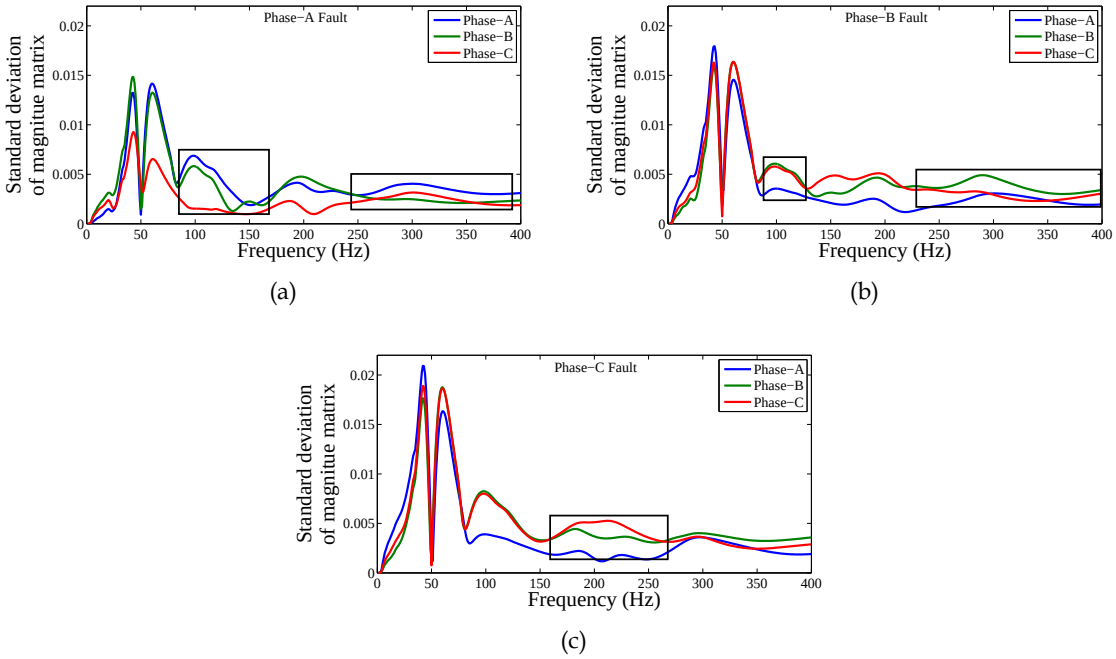

Figure 5.5 : Standard deviation of ST matrix of stator current signals along frequency axis under ground fault conditions when the fault is in (a) Phase-A, (b) Phase-B, and (c) Phase-C windings

by Equation 5.5:

$$F_n = \sum std(|S_j(\tau, f))||_{f_1,f_2,f_3} \tag{5.5}$$

where, $n = 1,2,3,..9$ is the index of 9 features, and $j = 1,2,3$ represent three-phases. In this way, each sample consists of nine features (three features for each phase). The details of the features are provided in Table 5.5. For the purpose of feature selection and classification, the same procedure

Table 5.5 : Feature list for Ground fault phase classification

Feature Name	Phase	Frequency range
F_1	A	f_1
F_2	A	f_2
F_3	A	f_3
F_4	B	f_1
F_5	B	f_2
F_6	B	f_3
F_7	C	f_1
F_8	C	f_2
F_9	C	f_3

is repeated as explained in Section 5.3.3.

5.4 RESULTS AND DISCUSSION

The current signals are decomposed using Stockwell transform to obtain complex 2D-matrices (ST matrices). These matrices reflect the variation of different frequencies (changed due to stator winding faults) with respect to time. Based on these matrices, a fault detection scheme is designed to detect the presence of fault, which can further detect the faulty phase in both turn-faults and ground-faults.

Figure 5.6 shows the standard deviation vector of a ST matrix of the current signals, calculated along frequency axis with respect to time for a frequency range of [1-400 Hz](above this range, no significant variations were observed). Figure 5.6 (a)- (c) show the SD for healthy, turn faults and ground faults conditions when the faulty phase is Phase-A, Phase-B, and Phase-C respectively. Evidently, there are high values of standard deviations at certain frequency ranges under fault conditions in comparison to healthy state. These changes in SD can be utilized to form a fault diagnostic algorithm for stator winding faults. For this purpose, SD of each phase current signal is calculated for a specified frequency ranges. For all three-phases, the values of SD are added in accordance with Equation 5.2 to determine fault index-1, FI_1 for all samples of turn-faults and ground faults. The mean values calculated for all samples of both fault types, with their respective error bars are shown in Figure 5.7.

Evidently, the value of this fault index is significantly low for healthy reference as compared to both fault cases. The high error bars reflect the standard deviation of these faults. Within the boundaries of the error bars, healthy is the lowest. Thus, the FI_1 of the reference healthy can be set as a threshold to compare FI_1 such that any value above this threshold would indicate the presence of fault.

Subsequent to the detection of fault, the other task is to identify the type of fault, i.e., turn-fault or ground fault. This step is done using fault index, FI_2 which is based on standard deviation of zero-sequence current for each sample of both fault conditions. The mean and

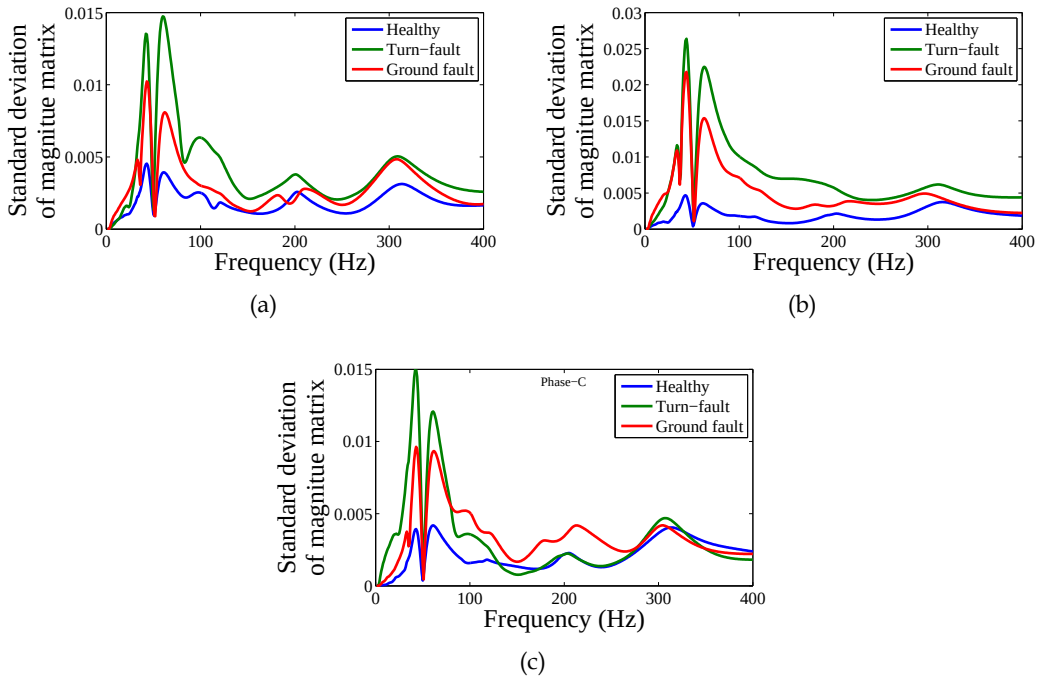

Figure 5.6 : Standard deviation of ST matrix of stator current signals along frequency axis for a healthy, turn-fault and ground fault condition in (a) Phase-A, (b) Phase-B, and (c) Phase-C

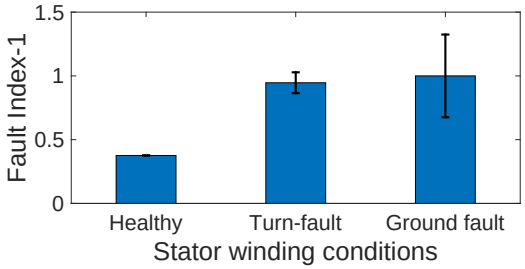

Figure 5.7 : Fault index for identifying faults in the stator windings

standard deviation values of all samples under both faults are shown in Figure 5.8. It can be observed that there is a significant difference in fault index, FI_2 for turn-shorts and ground faults. A threshold can be set as the mid value of the FI_2 for both faults. Post fault type detection i.e., turn-fault or ground fault, two SVM models, one for each are trained and tested. In the case of turn-faults, a total of 54 sets of samples are collected consisting all three-phase current signals. The sets comprises of signals with faults in one of the three phases. With this, three classes are defined for the classification purpose, i.e., phase-A, phase-B and phase-C, under which samples would be classified. For each class, a total of 18 samples are collected. For the classification, SVM classifier is used whose training is done using 36 samples (12 samples from each class) out of 54 samples. The remaining 18 samples (6 samples for each class) are used for testing purposes.

A multi-class SVM with One-Against-All approach is undertaken for classification purpose. Radial basis function is used as the kernel function on the basis of better performance than other kernels such as linear, polynomial etc. This is a widely used kernel on the fault diagnosis platform. The optimal values of the tuning parameters Gamma, γ which is width of the Gaussian function

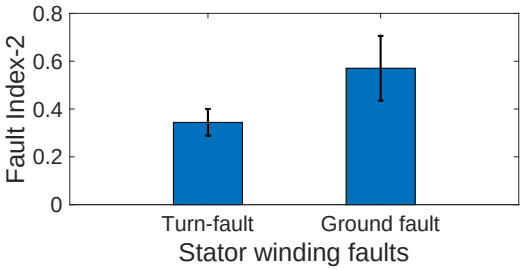

Figure 5.8 : Fault index for discriminating turn-faults and ground-faults in stator windings

and Cost, C which sets soft-margin in the classifier are determined using k-fold cross validation. Over the grid of γ and C, the training is performed and the pair of γ and C giving the highest average cross-validation accuracy is chosen. A heuristic approach is used to find the optimal features such that for every combination of features, the SVM-1 model is trained and validated. At first, the optimal values of C and γ are obtained and then the trained model with these values are tested on the unknown/testing dataset. For turn-faults, the cross validation is performed with $k = 4$. The maximum accuracy obtained under n feature combinations is shown in Figure 5.9. The combination of features giving the maximum accuracy is provided in Table 5.6. Thus, these six features from three-phases can be used for identification of faulty phase in turn-faults. The optimal values of $C = 2048$ and $\gamma = 0.004$ are found. The confusion matrix for this classification is provided in Table 5.7.

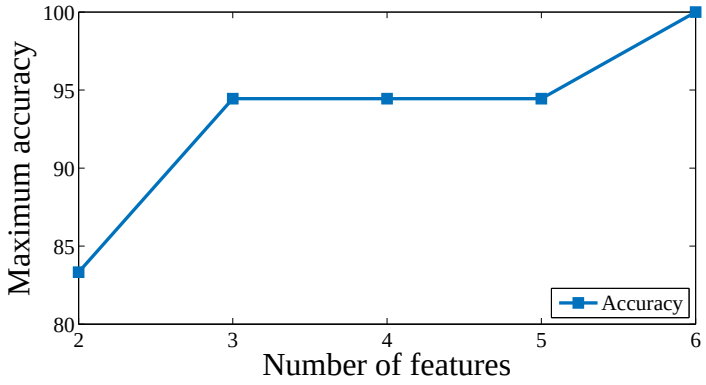

Figure 5.9 : Maximum accuracies for each set of feature combinations (n) for faulty phase detection in case of turn-faults

Table 5.6 : Features selected (giving highest accuracy) with each set of combinations for turn faults

Number of features (n)	Selected features	Accuracy (%)
2	f_1, f_4	83.33
3	f_3, f_4, f_8	94.44
4	f_1, f_3, f_6, f_9	94.44
5	f_1, f_2, f_3, f_4, f_8	94.44
6	$f_1, f_2, f_3, f_4, f_6, f_8$	100

For ground fault phase classification, a total of 189 samples are collected from the experiment, with 63 samples for each faulty phase. Out of 189 samples, 153 samples are used

Table 5.7 : Confusion matrix for SVM-1

	Phase-A	Phase-B	Phase-C	Class Accuracy (%)	Overall Accuracy
Phase-A	6	0	0	100%	100%
Phase-B	0	6	0	100%	
Phase-C	0	0	6	100%	

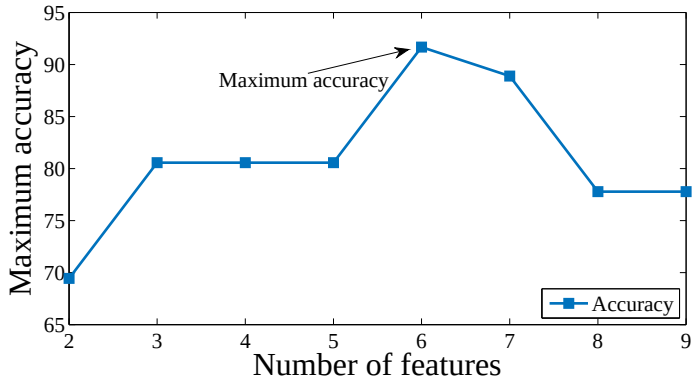

Figure 5.10 : Maximum accuracies for each set of feature combinations (n) for faulty phase detection in case of ground faults.

for training/validation and remaining 36 samples are used for testing purposes for SVM-2. Using Equation 5.5, nine features are determined for all samples. Similar, heuristic searching of optimal features as mentioned above is implemented here.For ground-faults, the cross validation is performed with $k = 10$.

Figure 5.10 shows the maximum accuracy obtained for $n = 1,2,3...9$ combinations of features to classify three classes. Thus, with six features as mentioned a classification accuracy of 91.66% is obtained with $C = 64$ and $\gamma = 0.5$. Table 5.8 shows the features giving the highest accuracy for each set of n. Table 5.9 shows the confusion matrix for the classification giving the highest accuracy.

Hence, with these features the faulty phase can be identified in case of ground faults. With this step, a complete algorithm is established which first identifies the presence of fault and the type, followed by detection of faulty phase in both cases using machine learning approach. The flowchart of the fault detection algorithm for stator winding faults is shown in Figure 5.11.

5.5 CONCLUSION

In this work, a fault detection, classification and location of stator winding faults in a three-phase induction motor is proposed. The stator current signals are decomposed using Stockwell transform, whose magnitude is statistically analysed. Standard deviation of the magnitude matrices is found to be useful for fault diagnosis purposes. A fault index is defined based on this parameter to identify the presence of fault (turn-fault or ground fault). Post fault detection, the aim is to identify the type of fault which is done with the help of zero sequence current based fault index. Subsequently, the identification of faulty phase is done using SVM models for both turn-faults and ground faults. These SVM models are trained with features

Table 5.8 : Features selected (giving highest accuracy) with each set of combinations for ground faults

Number of features (n)	Selected features	Accuracy (%)
2	f_1, f_4	69.44
3	f_3, f_5, f_9	80.55
4	f_2, f_3, f_5, f_8	80.55
5	f_1, f_2, f_5, f_7, f_9	80.55
6	$f_1, f_2, f_3, f_4, f_6, f_8$	**91.66**
7	$f_1, f_2, f_4, f_5, f_6, f_7, f_9$	88.89
8	$f_1, f_2, f_3, f_5, f_6, f_7, f_8, f_9$	77.78
9	ALL	77.78

Table 5.9 : Confusion matrix for SVM-2

	Phase-A	Phase-B	Phase-C	Class Accuracy (%)	Overall Accuracy
Phase-A	12	0	0	100%	91.66%
Phase-B	1	10	1	83.33%	
Phase-C	0	0	12	100%	

obtained from SD of magnitude matrix under pre-defined frequency ranges. A heuristic approach is used to obtain the best combination of features for classification. A k-fold cross validation is used to train and validate the SVM models, with $k = 4$ and $k = 10$ for turn-faults and ground faults respectively. An accuracy of 100% and 91.66% is obtained for turn-fault and ground fault respectively.

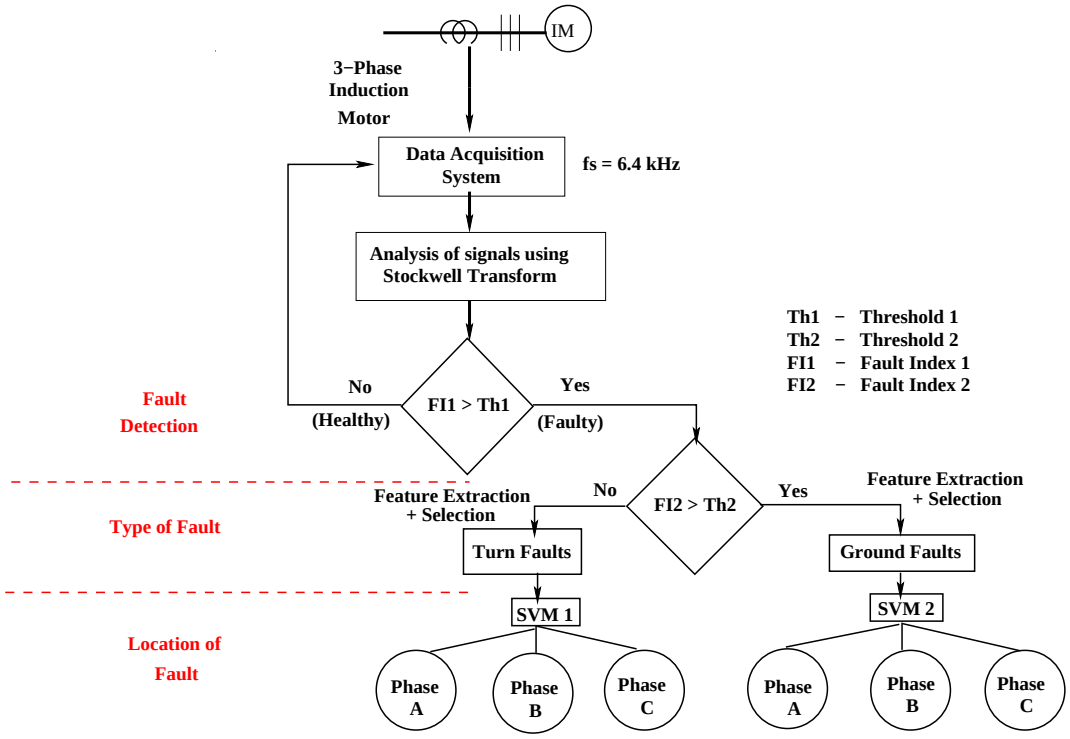

Figure 5.11 : Flowchart of the fault diagnosis strategy for stator winding faults